Surface & Coatings Technology 283 (2015) 115–121

Contents lists available at ScienceDirect

Surface & Coatings Technology

journal homepage: www.elsevier.com/locate/surfcoat

The influence of different silicon adhesion interlayers on the tribological behavior of DLC thin films deposited on steel by EC-PECVD

F. Cemin [a,*], L.T. Bim [a], C.M. Menezes [a], M.E.H. Maia da Costa [b], I.J.R. Baumvol [c], F. Alvarez [d], C.A. Figueroa [a,e]

[a] CCET, Universidade de Caxias do Sul, Caxias do Sul 95070-560, Brazil
[b] Departamento de Física, PUC-Rio, Rio de Janeiro 22453-900, Brazil
[c] IF, Universidade Federal do Rio Grande do Sul, Porto Alegre 91509-970, Brazil
[d] IFGW-DFA, Universidade Estadual de Campinas, Campinas 13083-970, Brazil
[e] Plasmar Tecnologia Ltda., Caxias do Sul 95076-420, Brazil

ARTICLE INFO

Article history:
Received 8 July 2015
Revised 21 September 2015
Accepted in revised form 17 October 2015
Available online 19 October 2015

Keywords:
DLC
Hydrogenated amorphous carbon
Hydrogenated amorphous silicon carbide
Adhesion interlayer
Nanoscratch test
Critical load

ABSTRACT

Diamond-like carbon (DLC) is a hydrogenated amorphous carbon (a-C:H) thin film material owing to its unique tribological properties that may open great opportunities for new applications. However, DLC presents low chemical affinity with metallic alloys and high intrinsic stress, prompting film delamination and poor adherence on the substrate. In the present work, we performed a systematic study about structural and tribological properties of a-C:H thin films grown on steel by introducing adhesive silicon-containing interlayers deposited at different processing temperatures and times. The studied bi-layers were deposited by electrostatic confinement plasma enhanced chemical vapor deposition (EC-PECVD) and were characterized by several techniques. The results showed that the adhesive interlayers produced from tetramethylsilane are chemically structured as a non-stoichiometry hydrogenated amorphous silicon carbide alloy (a-SiC_x:H). Its structure, chemical composition and thickness are very dependent on deposition conditions. The thickness of the interlayers increases with deposition time and decreases with deposition temperature. The interlayer contains less hydrogen and silicon atoms at higher deposition temperatures, with enhanced formation of Si–C bonds in its structure. This last chemical event is correlated with the rise in the critical load values found for a-C:H film delamination when the a-SiC_x:H interlayers are deposited from 573 K to 823 K. On the other hand, the interlayer contains less carbon atoms at higher deposition times, decreasing the critical load values for a-C:H film delamination when the a-SiC_x:H interlayers are deposited from 5 min to 10 min.

1. Introduction

Diamond-like carbon (DLC) is a hydrogenated amorphous carbon (a-C:H) thin film material that has attracted scientific interest and posterior industrial success because of its exceptional mechanical and tribological properties [1]. This material is currently used as a protective coating in automobile components, engine systems, fuel injectors, tool tips and razor blades mainly because of its low friction coefficient under dry sliding conditions and high wear resistance [2,3]. In order to improve the durability of DLC on tribological applications, films few micrometers thick are adequate [2]. In these cases, however, large compressive intrinsic stress arises, prompting film adhesive failures and delamination from the substrate surface [4,5]. Particularly when DLC is deposited on metallic alloys, the low chemical affinity, i.e., poor chemical bonding of carbon film to the substrate, also contributes to the spontaneous debonding effects.

Despite the several approaches available to improve the DLC film adhesion on metallic alloys, one can mention the deposition of intermediate metallic or ceramic layers between the substrate surface and the film, also called in most of works as *buffer layers*, adhesive interlayers or bonding interlayers [6,7,8,9,10,11]. Such layers mitigate the high compression by releasing stress, reduce structure film mismatching and promote stronger chemical bonds at the interfaces. In particular, silicon-containing interlayers are chemically more compatible to the material system studied, i.e., silicon has chemical affinity with the metallic atoms present in the alloy and with the carbon atoms constituting the DLC [2,11,12]. Despite the fact that the established use of silicon-containing interlayers in current industrial processes is a well known approach for improving DLC adhesion on steels, we did not find, in the specialized literature, works that investigate the influence of different deposition parameters for the Si-based interlayer (basically processing temperature and time) on the adhesion of DLC films on steels, by a systematic treatment of the results.

The improved adhesion of DLC films on metallic alloys by adhesive interlayers enhances the lifespan of the coating in tribological services, avoiding premature delamination under both higher loads and contact

* Corresponding author.
E-mail addresses: lipecemin@gmail.com, fcemin3@ucs.br (F. Cemin).

http://dx.doi.org/10.1016/j.surfcoat.2015.10.031
0257-8972/

pressures. Indeed, many tribological tests have shown that friction coefficients, wear rates and critical loads for delamination (the latter generally used to estimate the thin film adhesion) are influenced by the nature of the interlayer, besides factors such as thickness, Young's modulus and hardness of the coating, structural defects, topography and substrate characteristics [2]. Scratch and nanoscratch tests were reported in the specialized literature evaluating the DLC film adhesion on metallic alloys containing interlayers constituted by different chemical elements (e.g., Ti, Si, Cr, Cu, W, Mo, Nb), ceramic compounds and metal-carbides [6,13,14,15,16,17,18,19]. Despite the fact that most of these materials were able to improve DLC film adhesion on metallic alloys, the reported critical loads for delamination are pretty scattered. This is so because of the strong dependence on the interlayer characteristics and properties as well as the thin film characteristics. Indeed, each coated material system has its peculiarities (e.g., structural, chemical) making difficult offering unanimous recipes. Moreover, it should be considered that the DLC film, as well as the interlayer, is deposited in a variety of conditions and often from various chemical precursors. For the above reasons, a detailed scrutiny of the interlayer structure and properties has an important role on the optimization of DLC adhesion on metallic alloys for tribological applications where the lifetime of the coating is fundamental from both technical and economic reasons.

Therefore, this study is an attempt to establishing general physical and chemical indicators regarding DLC film adhesion on a ferrous alloy by intercalating a silicon-containing interlayer deposited from appropriated experimental conditions by electrostatic confinement plasma enhanced chemical vapor deposition (EC-PECVD). The friction coefficient and the critical load for DLC films delamination were evaluated by nanoscratch testing. In order to optimize the performance of the DLC coatings for tribological applications, these results are correlated with the structure, composition, and characteristics of the studied adhesive interlayers.

2. Materials and methods

The studied Si-based interlayers and DLC films were sequentially grown on a low-alloy steel (AISI 4140, composition in wt.%: C: 0.40, Cr: 0.96, Mo: 0.17, Si: 0.23, Mn: 0.85, Ni: 0.13, Cu: 0.15 and Fe: balance) by a EC-PECVD system. The electrostatic confinement applied for surface engineering is a relatively recent promising technology, and more details about the processes can be found elsewhere [20,21]. The samples were mirror polished using standard metallographic techniques and cleaned in ultrasonic bath with acetone before introducing them into the deposition chamber. The base pressure in the chamber was ≤1.5 Pa. For all the reported processes, the plasma was sustained by a negative pulsed direct current power supply (10 kHz) with a constant bias (+30 V) between the pulses, duty cycle of 40%. Prior to deposition, the substrates were cleaned by Ar^+ ion plasma bombarding (30 min, at 10 Pa chamber pressure and at −500 V applied voltage). Then, the adhesive silicon-containing interlayers were prepared from a vapor mixture of tetramethylsilane (TMS, $Si(CH_3)_4$) and Ar (~80%–20% partial pressure, respectively) at a total pressure of 60 Pa. Liquid TMS was heated and evaporated at 313 K by using a controlled evaporator and mixer device (Bronkhorst High-Tech B.V.). In the first group of studied samples, the substrate temperature was varied from 373 K to 823 K by using a resistive heating, with the deposition time maintained constant for 10 min for the different samples. In the second group of studied samples, the interlayer deposition time was varied from 1 min to 10 min, with the substrate temperature maintained constant at 573 K for the different samples. The glow discharge was sustained applying a voltage of −500 V during this stage. Finally, DLC films were deposited on the top of the different interlayers under the same experimental conditions for all the studied samples, using a gaseous mixture of acetylene (C_2H_2) and Ar, flow rates of 13 and 4 sccm, respectively, at 10 Pa total pressure. The glow discharge was sustained applying a voltage of −800 V for 60 min at ~353 K. In addition, some samples were prepared without posterior DLC deposition in order to study the chemical structure of the silicon-containing interlayer deposited at different temperatures.

The morphology, microstructure and thickness of the bi-layers were investigated by SEM — Shimadzu SSX-550, by analyzing the cross-section of the samples. In depth chemical profiles of the samples were obtained by GDOES — Horiba GD-Profiler 2. Structural details of DLC films and silicon-containing interlayers were analyzed by Raman scattering spectroscopy — Raman Confocal NTegra Spectra NT-MDT, 473 nm laser. The tribological properties of DLC thin films were evaluated by using a nanoindentation system — Micro Materials NanoTest-600, equipped with a conical diamond tip with final radius of 25 μm. A normal load of 0.01 mN was applied in the firsts 100 μm of the scan and then the load was linearly ramped at 0.3 mN s^{-1} up to reach a final normal load of 500 mN, as the tip was dragged through a distance of 1800 μm over the sample surface. During the nanoscratch test, the normal load, penetration depth, lateral (friction) forces and friction coefficient were continuously monitored. The critical load (Lc) for delamination was defined as the minimum normal load which can cause the initiation of film delamination from the surface, followed by an abrupt variation in lateral force and friction coefficient. Five scratch tracks were performed in each sample to determine an average value of Lc. After testing, the surface examination was carried out by optical microscopy (OM) and SEM to verify the failure modes of the films along the scratch tracks.

3. Results and discussion

Fig. 1 presents a schematic combination of SEM cross-section image and GDOES analysis results for the sample where the silicon-containing interlayer was deposited at 673 K during 10 min between the steel and

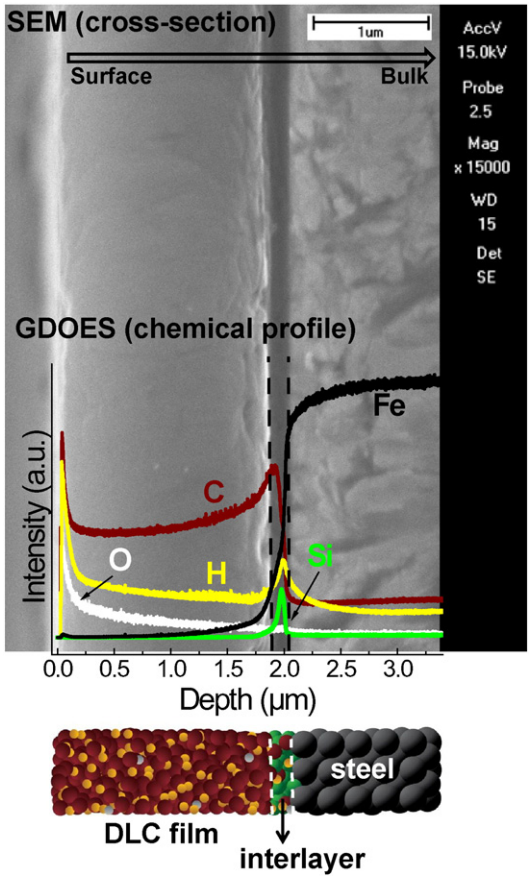

Fig. 1. In-depth chemical profile obtained by GDOES superimposed on a cross-section SEM image for the sample with the interlayer deposited at 673 K during 10 min between the steel and the DLC film. A schematic illustration of the material system is also shown.

the DLC film. The observed behavior is typical for all samples studied in this work, comprising two well-defined layers and the substrate. Initially, from left to right, the outermost layer is a microstructured material containing a relative high signal of carbon and hydrogen, which characterizes it as the DLC thin film. Subsequently one can notice the presence of a submicrometric layer containing a relative high signal of carbon, hydrogen and silicon, which typifies it as the adhesive silicon-containing interlayer. Both film and interlayer presents a residual relative signal of oxygen, which arises probably from oxygen and water vapor adsorbed in the deposition system. Finally, the ferrous alloy is visualized in the region containing a relative high signal of iron. In addition, a schematic representation in chemical terms of the material system described above is included at the bottom of the main figure.

The DLC film presents a quite uniform average thickness of 1.8 ± 0.2 μm in all studied samples. These films were produced following exactly the same experimental conditions, thus, we expected to obtain similar values of thickness and evenness in all studied samples. Meanwhile, the thickness of the silicon-containing interlayer depends on both the deposition time and temperature. Fig. 2 shows the interlayer thickness evolution as a function of substrate temperature (maintaining the time deposition time constant at 10 min) and deposition time (maintaining the substrate temperature constant at 573 K). One can see that the interlayer thickness exponentially decreases on increasing the deposition temperature, from 831 nm (373 K) to 133 nm (823 K), following a thermally activated kinetic process, as already reported in a previous work [11]. In contrast, the interlayer thickness augments on increasing the deposition time, in a much less remarkable behavior, from 150 nm (1 min) to 318 nm (10 min). Such a thickness increase on augmenting the deposition time is due to the accumulation of deposited material over time.

Fig. 3 shows the C/H and Si/C content ratios in the interlayer structure as a function of substrate temperature and deposition time, obtained from area measurements under carbon, silicon and hydrogen GDOES profiles for each studied sample in the interlayer region. Once again, an inverse behavior is observed as a function of the two studied variables. On the one hand, C/H ratio increases on augmenting the deposition temperature and does not appreciable change on augmenting the deposition time. On the other hand, Si/C ratio decreases on augmenting the deposition temperature and increases on augmenting the deposition time. Regarding to the temperature effect on the interlayer chemical composition, the increase of the C/H ratio could mean that the interlayer contains less hydrogen when it is grown at higher temperatures, and the decrease of the Si/C ratio could mean that the interlayer contains less silicon when it is grown at higher temperatures. The

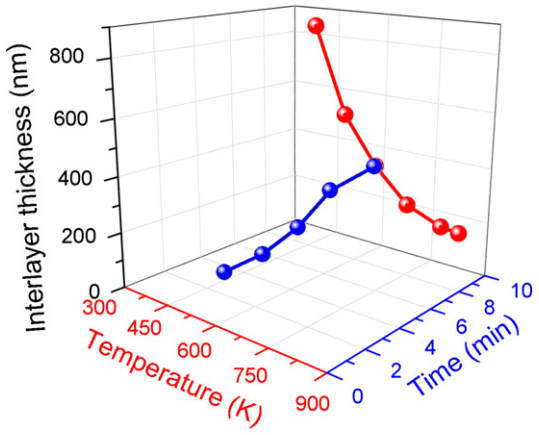

Fig. 2. Interlayer thickness as a function of the deposition time (at a constant substrate temperature of 573 K) and the substrate temperature (at a constant deposition time of 10 min), deposited between the steel and the DLC film. The thickness measurements were carried out directly from SEM images in cross-section.

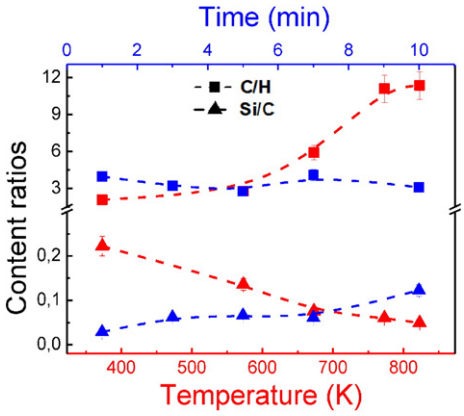

Fig. 3. C/H and Si/C content ratios in the silicon-containing interlayer as a function of deposition time and substrate temperature. The values were obtained by the integration of the area under the specific GDOES profiles in the interlayer region for each sample.

hydrogen and silicon losses may be related with diffusion or desorption processes during interlayer growth. In order to analyze the occurrence of diffusion process, Fig. 4 shows the in-depth GDOES chemical profiles of (a) hydrogen and (b) silicon at different interlayer deposition temperatures. One can see that both hydrogen and silicon profiles do not appreciable change in the steel region at higher deposition temperatures. It suggests that these atoms do not diffuse into the bulk material and may be desorbed from the interlayer during growth process at higher deposition temperatures. The thermal energy can activate chemical reactions at the surface and subsurface of the interlayer during growth process, favoring the formation of volatile chemical species containing silicon and/or rich in hydrogen (such as silane, molecular hydrogen and vapor water), that can be transferred to the gas phase during film growth. Indeed, many works have demonstrated that hydrogen is released from the structure of silicon-containing films at higher deposition temperatures [22,23]. Also, the desorption phenomenon could be contributing to the interlayer thickness decrease at higher deposition

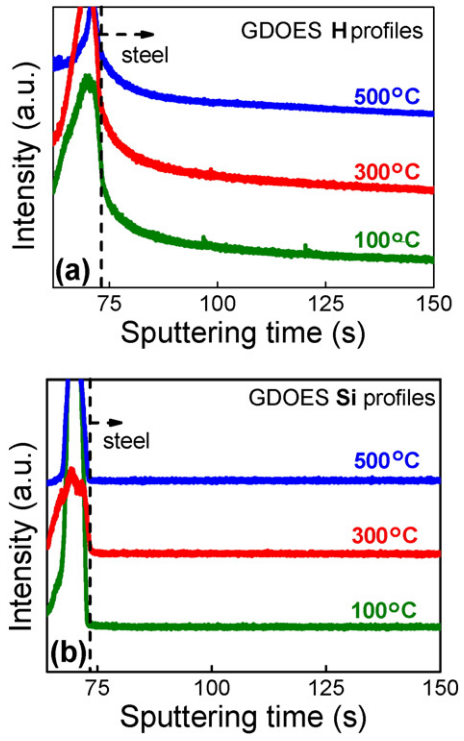

Fig. 4. (a) Hydrogen and (b) silicon in-depth profiles obtained by GDOES for the interlayers deposited at different substrate temperatures. Sputtering time is proportional to depth.

temperatures, as previously observed in Fig. 2. Finally, regarding to the deposition time effect on the interlayer chemical composition, the increase of the Si/C ratio could mean that less carbon is present in the samples with the interlayer deposited at longer times. Such a physical-chemical phenomenon could be related with chemical reactions occurring during interlayer growth responsible for releasing, for example, CH^+ species (once C/H ratio remains constant for all studied samples) from the interlayer structure. This chemical event seems to be very dependent on time, and absent on temperature, in the studied ranges.

Fig. 5 shows a typical Raman spectrum of the DLC film surface from one of the studied samples, with the characteristics D (disorder) and G (graphite) bands centered at ~1355 cm^{-1} and 1550 cm^{-1}, respectively. The bands were fitted using two Gaussian distributions and a linear background. The broad peaks in Fig. 5 reflect the inhomogeneous broadening (disorder) characteristic from the amorphous nature of the material, being similar to those found in a-C:H films [1]. The G-peak positions and I_D/I_G ratios of the different samples studied are similar (not shown) because, as noted above, the same experimental conditions were used on depositing the a-C:H films. Then, one can conclude that the film structure is not influenced by the different silicon-containing interlayers.

In the attempt to understand the chemical bonding present in the interlayer, Fig. 6 shows the selected Raman spectra of the silicon-containing interlayers deposited at different substrate temperatures, varying from 373 K to 773 K, without posterior a-C:H film deposition. Initially, one can see that increasing the temperature during the interlayer deposition, the intensity of all peaks increases, i.e., a better structure organization is achieved at higher temperatures. We remark that increasing inhomogeneous broadening is found in all deposition temperatures, which are characteristic of highly disordered (amorphous) structures. For comparison effects, two spectra were inserted at the top of Fig. 6: a pure amorphous silicon (a-Si) film [24] and a tetrahedral amorphous carbon (ta-C) film [1]. Our spectra exhibit Si–Si vibration modes centered around ~480 cm^{-1} and ~1000 cm^{-1}, being the first one related to a-Si and the last one related to a second-order Si–Si mode that corresponds to the presence of amorphous silicon carbide (a-SiC) [25,26]. Also, one can identify a broad feature at ~800 cm^{-1}, corresponding to Si–C vibration mode, as expected for an a-SiC alloy [2,26]. Finally, it is possible to observe a broad peak in ~1480 cm^{-1}, associated with carbon clusters either in diamond-like or graphite-like bonding modes, and a broad peak at ~2100 cm^{-1}, associated with the Si–H_n vibration mode [25,26]. These results show that the silicon-containing interlayer is chemically structured as a non-stoichiometry hydrogenated amorphous silicon carbide alloy (a-SiC_x:H), very dependent on the deposition temperature. At 373 K, the interlayer is not structurally speaking quite well defined, with no Si–Si or Si–C vibration modes detected by Raman analysis. The absence of such vibration modes, i.e., such bonds in the structure, could be associated

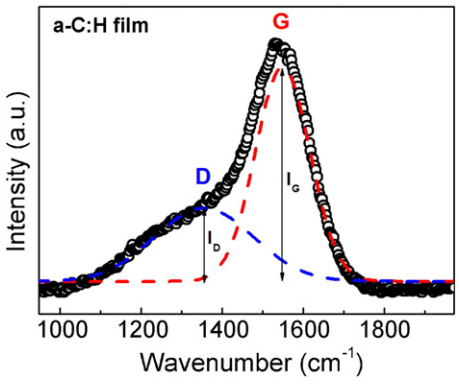

Fig. 5. Raman spectrum for the DLC film deposited on the interlayer grown at 573 K during 10 min on steel.

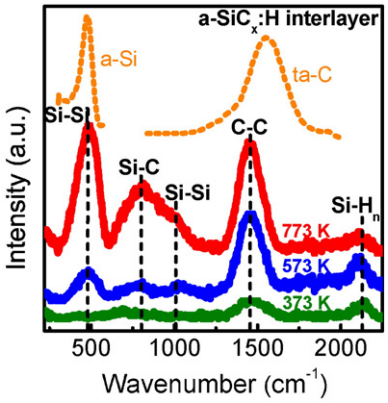

Fig. 6. Raman spectra for the a-SiC_x:H interlayers deposited at different temperatures, without posterior a-C:H deposition.

with the large presence of residual hydrogen and oxygen atoms acting as terminators of silicon and carbon bonds, preventing the formation of strong C–C, Si–C and Si–Si bonds. At temperatures of 573 K and 773 K, the structure presents relative high intensity bands associated with C–C, Si–C and Si–Si bonds, which are compatible to those found in a-SiC:H alloys, and the intensity of Si–H_n is lower. Besides that, the temperature increase leading to an increase of Si–C bonds seems to augment the disorder of the structure, because the irregular distribution of Si–C bonds contributes to additional bond angle distortion and consequently increasing the inhomogeneous broadening of the Raman spectra [27].

The use of such a configuration, i.e., a material system composed by the steel/interlayer/DLC sandwich structure is capable to improve DLC films adhesion on steel. Fig. 7 shows an image of the surface characteristics of three selected samples. Initially, the sample on the left shows the polished surface of the AISI 4140 plain steel (for comparison effects). After, the sample on the middle shows the plain steel coated with DLC film without the presence of any adhesion interlayer. One can clearly see a gross delamination of the DLC film from the steel surface; the film without any interlayer immediately delaminates after deposition process. This spontaneous cracking is characteristic of seriously stressed films that break down in contact with the atmosphere and/or temperature shock. Finally, the sample on the right in Fig. 7 shows the plain steel coated with DLC film in the presence of the a-SiC_x:H interlayer deposited at 673 K for 10 min. One can notice the presence of a dark film qualitatively adhered on the surface of the steel sample, with visual characteristics really close to those found in a-C:H films. Thus, it is possible to claim that a-SiC_x:H interlayers enhance the delamination resistance of DLC films on steels. However, we will show hereafter that the quality of the observed improved DLC adhesion is extremely influenced by the experimental conditions used during interlayer growth process. The deposition parameters variation modifies the interlayer thickness, chemical composition and chemical structure (as previously shown) with consequent impact on DLC films adhesion.

In order to correlate the study performed theretofore with the a-C:H thin films adhesion on the a-SiC_x:H interlayers deposited from appropriated experimental conditions on steel, the studied samples undergo some qualitative and semi-quantitative tests for adhesion evaluation. Initially, the adhesion was qualitatively evaluated by macroscopic verification and tape peel tests. Regarding to the interlayer deposition temperature effect, the a-C:H films do not show spontaneous delamination for a-SiC_x:H interlayers deposited at temperatures between 573 K and 823 K [11]. At lower interlayer deposition temperatures (373 K and 473 K), the a-C:H films showed deleterious effects of spallation and spontaneous delamination, preventing further analysis of samples by nanoscratch testing. The chemical effect that contributes to the spontaneous delamination of a-C:H films on a-SiC_x:H interlayers deposited on steel at 373 K and 473 K was reported in a previous work [28], and it is

Fig. 7. Surface characteristics of the AISI 4140 plain steel polished (on the left), the AISI 4140 plain steel coated with DLC film without any adhesion interlayer (on the middle) and the AISI 4140 plain steel coated with DLC film in the presence of the a-SiC_x:H adhesion interlayer deposited at 673 K for 10 min (on the right).

related with the excessive presence of hydrogen and oxygen on the interlayer structure. These atoms act as terminators of silicon and carbon dangling bonds, preventing the formation of strong covalent bonds at the a-SiC:H/a-C:H interface between carbon and silicon atoms from the interlayer and carbon atoms from the a-C:H film. Regarding to the interlayer deposition time effect, no spontaneous delamination was observed for the samples deposited from 1 min to 10 min at a constant temperature of 573 K. Thus, all samples that showed no spontaneous delamination and deleterious effects were submitted to nanoscratch testing.

Fig. 8 shows a schematic composition of the results obtained from nanoscratch testing for the sample with the a-C:H film deposited on the a-SiC_x:H interlayer grown at 673 K during 10 min on steel (sample on the right in Fig. 7). The scratching curves and surface images were used to study the tribological properties (such as friction coefficient and critical load for delamination) of the a-C:H films studied. Fig. 8a shows a typical behavior of the normal load (on the left) and the lateral load – or frictional force – (on the right) plotted together as a function of the scratch distance. While the normal load increases linearly from 0 to 500 mN, the lateral load increases monotonically up to ~100 mN, characteristic from a plastic deformation, with no cracks or delamination. At such critical force, corresponding at a normal load slightly above of ~400 mN, a serious delamination process is initiated and propagated up to the end of the scratch distance. Therefore, this event characterizes the normal load of 418 ± 9 mN as the critical one for prompting delamination of a-C:H film when the a-SiC_x:H interlayer is grown on steel at 673 K. Fig. 8b shows a surface image of the scratching tracks obtained by OM in such studied sample, which highlights the starting point of the plastic deformation (Lc_1) and the beginning of the delamination process (Lc_2). The measured friction coefficient of the studied sample was continuously monitored during the nanoscratch test, as shown in Fig. 8c. The friction coefficient increases from ~0.02 to ~0.2 as the normal load increases from 0 mN to ~400 mN (at the beginning of the delamination process). Our scratch tests were performed at variable normal load. Therefore, the rise of the friction coefficient is due to larger real contact areas at higher normal loads (before delamination) and the surface damage during the delamination. The delaminated film and the wear track create new forces where some of them are not only tangential but also perpendicular to the diamond tip displacement plane, which increase more the lateral force in a very short period of time (sharp shape). Due to this effect, we choose to evaluate the friction coefficient for all the studied samples at a fixed scratch distance of 500 μm, which corresponds also to the same normal load. Following this criterion, an average value equal to 0.05 ± 0.02 at a normal load of 120 mN was found. This friction coefficient value is similar to those ones generally reported for a-C:H films [2] under dry sliding conditions.

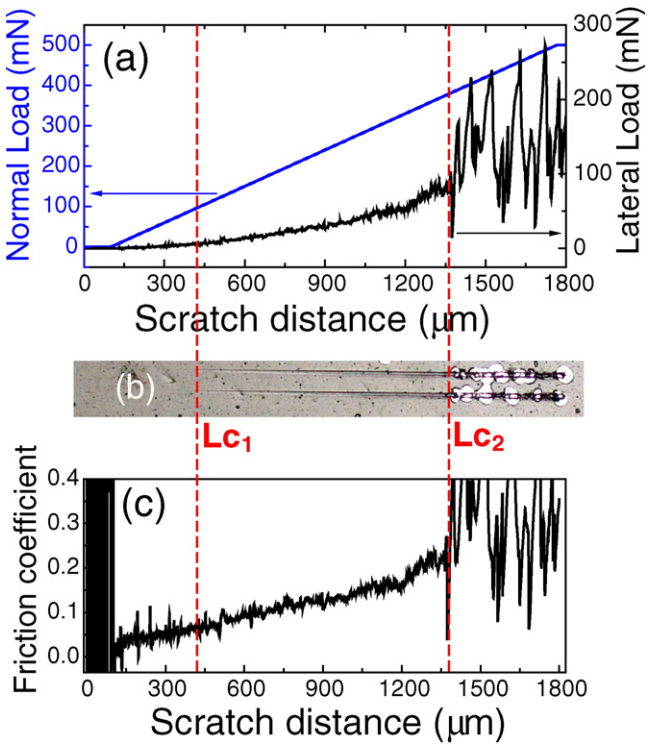

Fig. 8. Association of results obtained from nanoscratch testing for the a-C:H film with the interlayer deposited at 673 K during 10 min: (a) evolution of the normal load (on the left) and the lateral load (on the right) as a function of scratch distance; (b) OM image from the surface of the scratch tracks, demonstrating the critical loads for plastic deformation (Lc_1) and delamination (Lc_2); and (c) friction coefficient as a function of scratch distance.

Fig. 9 shows SEM images of two specific regions in the same nanoscratch track of the sample with the interlayer grown at 673 K for 10 min between the a-C:H film and steel. The SEM images demonstrate the typical surface damage and fracture behavior of the a-C:H films submitted to nanoscratch testing. Fig. 9a shows the microstructural appearance of the scratch track just before the film fracture. One can see the presence of arc tensile cracks and conformal cracks into the scratched area, although there is no delamination of the film when the applied normal load increases from 0 to ~418 mN. When the critical load for delamination (Lc_2 — 418 mN) is reached, the thin film is firstly ruptured, as shown in Fig. 9b. The fracture leads to film gross spallation across the scratch track, extending the delamination process to the unscratched area due to film chipping. The detailed microstructure of the point at which the critical load for delamination is reached is presented at the region highlighted.

The critical load for delamination was evaluated for all samples that have demonstrated no spontaneous a-C:H film delamination. Such a property is commonly used as a semi-quantitative measurement of thin films practical adhesion. Fig. 10a shows the values of critical load for film delamination as a function of interlayer deposition temperature, maintaining the deposition time fixed at 10 min. One can see that the a-C:H film adhesion depends on the a-SiC_x:H deposition temperature; the critical load for film delamination is monotonically enhanced from

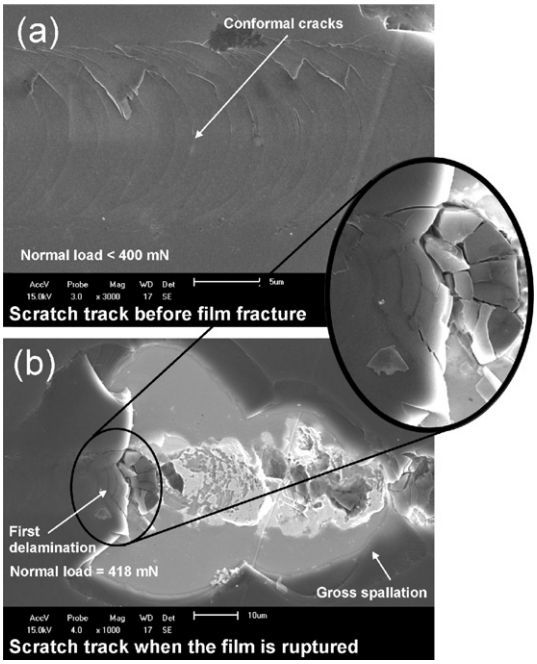

Fig. 9. SEM images of the scratch track (a) just before the thin film fracture and (b) on the first rupture and delamination of the a-C:H film. The enlarged region shows the exact point where the critical load for delamination is reached. The interlayer was deposited at 673 K during 10 min between the steel and the DLC film.

298 mN (at 573 K) to 470 mN (at 823 K). As we have previously demonstrated, the deposition temperature influences on the interlayer thickness, structure and chemical composition, and these changes could be related with the improved behavior in the critical load values observed in Fig. 10a. Although there are several physical, mechanical and tribological factors affecting the adhesion strength, we suggest that a chemical factor can also contribute to or deteriorate the a-C:H film adhesion on steels intermediated by a a-SiC_x:H interlayer. Thereby, at higher deposition temperatures, the adhesion interlayer presents a chemical structure with a preferable silicon carbide formation due to the thermal desorption of hydrogen and residual molecules as oxygen and water vapor. Also, the interlayer is richer in carbon atoms when deposited at higher temperatures. These chemical changes introduced by the deposition temperature modify the outermost interface of the interlayer (a-SiC_x:H/a-C:H interface), enhancing the a-SiC_x:H chemical affinity with the a-C:H film through more C–C chemical bonds between the film and the interlayers deposited at higher temperatures. The enhanced chemical affinity in the outermost interface could improve the adhesion strength, contributing to the observed increase in the critical load for delamination.

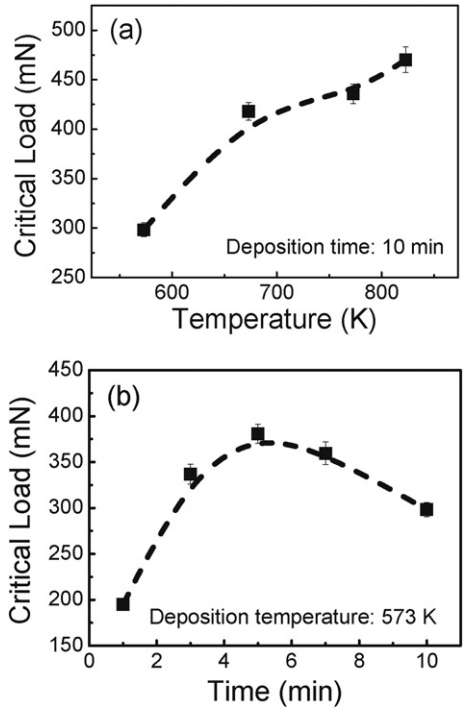

Fig. 10. Critical loads for a-C:H thin film delamination as a function of (a) interlayer deposition temperature and (b) interlayer deposition time.

Fig. 10b shows the values of critical load for film delamination as a function of interlayer deposition time, maintaining the substrate temperature constant at 573 K. One can see that the a-C:H film adhesion depends on the a-SiC_x:H deposition time and the critical load for films delamination reaches a maximum value of 381 mN for a deposition time of 5 min. Either for deposition times shorter or longer than 5 min, the critical load for delamination decreases. Indeed, two different and opposite mechanisms are governing the critical load for delamination as a function of the interlayer deposition time at a constant temperature of 573 K. For shorter deposition times, the critical load for delamination increases when the interlayer deposition time increases from 1 to 5 min, i.e., when the interlayer thickness increases from ~149 to ~198 nm. Although our adhesion mechanism considers a chemical approach, we have also to consider the mechanical strength of the system as a whole. For the material system studied in this work, with a DLC film ~1.8 μm thick, an interlayer 198 nm thick exhibited the best critical load value. Thus, the critical loads increase for the interlayers grown from 1 to 5 min because of a minimum interlayer thickness is necessary to achieve a minimum mechanical strength of the system. For interlayers thicker than the minimum interlayer thickness for mechanical strength (deposition times longer than 5 min), we suggest that the adhesion is controlled by the chemical bonding. This last tribological event is correlated with an interlayer that contains more silicon than carbon atoms (please, see the Si/C ratio in Fig. 3), which may deteriorate the adhesion at the atomic level due to the fact that Si–Si chemical bonds are weaker than C–C sp^3 chemical bonds [11].

4. Conclusions

A comprehensive study of the critical load for delamination of a-C:H thin films was performed as a function of structure, chemical composition and thickness of adhesive a-SiC_x:H interlayers deposited from TMS by EC-PECVD on steel at variable processing times and temperatures. On the one hand, the increase in deposition temperature exponentially decreases the interlayer thickness and induces hydrogen and silicon thermal desorption during interlayer growth process. The preferential formation of Si–C bonds on the interlayer enhances the a-SiC_x:H chemical affinity with the a-C:H film, contributing to improve the thin film adhesion (the critical load values for delamination) when the interlayer is grown in temperatures ≥573 K. On the other hand, the increase in deposition time augments the interlayer thickness and induces carbon losses, diminishing the a-SiC_x:H chemical affinity with the a-C:H film and its adhesion strength. The observed improved adhesion of a-C:H films on the studied ferrous alloy by the intercalation of a-SiC_x:H interlayers deposited in optimized experimental conditions could come to enhance the lifespan of the coated components in devices submitted to tribological services, avoiding faster delamination and deterioration of the coating. Also, the chemical phenomena proposed in this work can contribute to explain the adhesion in the system composed by the steel/interlayer/DLC sandwich structure and could be used in conjunct with the well established mechanical, physical and tribological phenomena.

Acknowledgments

The authors are grateful to UCS, INCT-INES (#554336/2010-3), CAPES (Brafitec 087/11), FAPERGS, CNPq-PETROBRAS (#166687/2014-6) and Plasmar Tecnologia Ltda. for financial support. FC, LTB, CMM, MEHMC, IJRB, FA, and CAF are CNPq and CAPES fellows. FC is in part supported by PETROBRAS (#166687/2014-6). FA is in part supported by FAPESP project (2012/10127-5). This work was supported by the SUMA2 Network Project, 7th Framework Program of the European Commission (IRSES Project # 318903).

References

[1] J. Robertson, Diamond-like amorphous carbon, Mater. Sci. Eng. R 37 (2002) 129–281.
[2] C. Donnet, A. Erdemir (Eds.), Tribology of Diamond-lie Carbon Films: Fundamentals and Applications, Springer, New York, 2008.
[3] K. Bewilogua, D. Hofmann, History of diamond-like carbon films — from first experiments to worldwide applications, Surf. Coat. Technol. 242 (2014) 214–225.
[4] C.A. Davis, A simple model for the formation of compressive stress in thin films by ion bombardment, Thin Solid Films 226 (1993) 30–34.
[5] D. Nir, Energy dependence of the stress in diamondlike carbon films, J. Vac. Sci. Technol. A 4 (1986) 2954–2955.
[6] K.-R. Lee, K.Y. Eun, I. Kim, J. Kim, Design of W buffer layer for adhesion improvement of DLC films on tool steels, Thin Solid Films 377–378 (2000) 261–268.
[7] C.-L. Chang, D.-Y. Wang, Microstructure and adhesion characteristics of diamond-like carbon films deposited on steel substrates, Diamond Relat. Mater. 10 (2001) 1528–1534.
[8] C.-C. Chen, F.C.-N. Hong, Interfacial studies for improving the adhesion of diamond-like carbon films on steel, Appl. Surf. Sci. 243 (2005) 296–303.
[9] C. Wei, C.-H. Chen, The effect of thermal and plastic mismatch on stress distribution in diamond like carbon film under different interlayer/substrate system, Diamond Relat. Mater. 17 (2008) 1534–1540.
[10] C. Wei, Y.-S. Wang, F.-C. Tai, The role of metal interlayer on thermal stress, film structure, wettability and hydrogen content for diamond like carbon films on different substrate, Diamond Relat. Mater. 18 (2009) 407–412.
[11] F. Cemin, L.T. Bim, C.M. Menezes, C. Aguzzoli, M.E.H. Maia da Costa, I.J.R. Baumvol, F. Alvarez, C.A. Figueroa, On the hydrogenated silicon carbide (SiC_x:H) interlayer properties prompting adhesion of hydrogenated amorphous carbon (a-C:H) deposited on steel, Vacuum 109 (2014) 180–183.
[12] S. Neuville, A. Matthews, A perspective on the optimisation of hard carbon and related coatings for engineering applications, Thin Solid Films 515 (2007) 6619–6653.
[13] M.D. Bentzon, K. Mogensen, J.B. Hansen, C. Barholm-Hansen, C. Traeholt, P. Holiday, S.S. Eskildsen, Metallic interlayers between steel and diamond-like carbon, Surf. Coat. Technol. 68–69 (1994) 651–655.
[14] Y. Jun, J.-Y. Choi, K.-R. Lee, B.-K. Jeong, S.-K. Kwon, C.-H. Hwang, Application of diamond-like carbon films to spacer tools for electron guns of cathode ray tube (CRT), Thin Solid Films 377–378 (2000) 233–238.
[15] M. Azzi, P. Amirault, M. Paquette, J.E. Klemberg-Sapieha, L. Martinu, Corrosion performance and mechanical stability of 316L/DLC coating system: role of interlayers, Surf. Coat. Technol. 204 (2010) 3986–3994.
[16] Z.-H. Xie, R. Singh, A. Bendavid, P.J. Martin, P.R. Munroe, M. Hoffman, Contact damage evolution in a diamond-like carbon (DLC) coating on a stainless steel substrate, Thin Solid Films 515 (2007) 3196–3201.
[17] T.H. Zhang, Y. Huan, Nanoindentation and nanoscratch behaviors of DLC coatings on different steel substrates, Compos. Sci. Technol. 65 (2005) 1409–1413.
[18] L.-Y. Huang, K.-W. Xu, J. Lu, Evaluation of scratch resistance of diamond-like carbon films on Ti alloy substrate by nano-scratch technique, Diamond Relat. Mater. 11 (2002) 1505–1510.
[19] M. Xu, L. Li, X. Cai, Y. Liu, Q. Chen, P.K. Chu, Improvement of adhesion strength of amorphous carbon films on tungsten ion implanted 321 stainless steel substrate, Diamond Relat. Mater. 15 (2006) 952–957.
[20] S.C. Gallo, A.E. Crespi, F. Cemin, C.A. Figueroa, I.J.R. Baumvol, Electrostatically confined plasma in segmented hollow cathode geometries for surface engineering, IEEE Trans. Plasma Sci. 39 (2011) 3028–3032.
[21] S.M.M. Dufrène, F. Cemin, M.R.F. Soares, C. Aguzzoli, M.E.H. Maia da Costa, I.J.R. Baumvol, C.A. Figueroa, Hydrogenated amorphous carbon thin films deposition by pulsed DC plasma enhanced by electrostatic confinement, Surf. Coat. Technol. 258 (2014) 219–224.
[22] V.I. Ivashchenko, S.N. Dub, O.K. Porada, L.A. Ivashchenko, P.L. Skrynskyy, A.I. Stegniy, Mechanical properties of PECVD a-SiC:H thin films prepared from methyltrichlorosilane, Surf. Coat. Technol. 200 (2006) 65338–66537.
[23] M.A. Bayne, Z. Kurokawa, N.U. Okorie, B.D. Roe, L. Johnson, Microhardness and other properties of hydrogenated amorphous silicon carbide thin films formed by plasma-enhanced chemical vapor deposition, Thin Solid Films 107 (1983) 201–206.
[24] S.V. Gaisler, O.I. Semenova, R.G. Sharafutdinov, B.A. Kolesov, Analysis of Raman spectra of amorphous nanocrystalline silicon films, Phys. Solid State 46 (2004) 1528–1532.
[25] A. Chehaidar, R. Carles, A. Zwick, C. Meunier, B. Cros, J. Durand, Chemical bonding analysis of a-SiC:H films by Raman spectroscopy, J. Non-Cryst. Solids 169 (1994) 37–46.
[26] W.K. Choi, Optical, structural, and electrical properties of amorphous silicon carbide films, in: H.S. Nalwa (Ed.), Silicon-Based Materials and Devices, Academic Press, Burlington 2001, pp. 2–71.
[27] D.M. Bhusari, R.O. Dusane, S.T. Kshirsagar, Properties of a-$Si_{1-x}C_x$:H alloys deposited in the hot-plasma — box glow discharge reactor, J. Non-Cryst. Solids 137–138 (1991) 689–692.
[28] F. Cemin, L.T. Bim, L.M. Leidens, M. Morales, I.J.R. Baumvol, F. Alvarez, C.A. Figueroa, Identification of the chemical bonding prompting adhesion of a-C:H thin films on ferrous alloy intermediated by a SiC_x:H buffer layer, ACS Appl. Mater. Interfaces 7 (2015) 15909–15917.